https://doi.org/10.2478/acph-2025-0013

Original research paper

Development of two different eco-friendly label-free platforms for analysis of selumetinib

SARAH ALRUBIA
WAFA A. ALSHEHRI
NOURAH Z. ALZOMAN
IBRAHIM A. DARWISH*

Department of Pharmaceutical Chemistry, College of Pharmacy
King Saud University, Riyadh, Saudi Arabia

*Correspondence; e-mail: idarwish@ksu.edu.sa

ABSTRACT

Selumetinib (SEL) is a recently approved medication for paediatric patients who have neurofibromatosis type-1. It is the first approved therapy for this rare, debilitating and disfiguring disease. Development of proper analytical platforms for SEL analysis in its marketed pharmaceutical formulation (Koselugo®capsules) and blood plasma is highly warranted. Availability of such analytical tools would ensure SEL capsules quality and effective therapy. This study introduces, for the first time, the development of two label-free and sensitive platforms for SEL quantification in capsules and human plasma. These platforms are microwell-assisted with ultraviolet absorbance microplate reader (MW-UV) and reverse-phase high-performance liquid chromatography with photodiode-array detector (HPLC-PDA). Both platforms employed the SEL native UV absorption as an analytical signal. The MW-UV measured the UV absorption in 96-well transparent plates at 255 nm. The HPLC-PDA involved chromatographic separation of SEL and tozasertib (TOZ), internal standard, on C18-column; both were detected at 255 nm. The optimum procedures of both platforms were established and validated following the ICH guidelines. The linearity ranges were 15-500 μg mL^{-1} and 0.8-100 μg mL^{-1}, with limits of quantification of 15.3 and 3.5 μg mL^{-1}, for MW-UV and HPLC-PDA, resp. Both platforms displayed high precision with relative standard deviation values ≤1.8 %, and high accuracy

with recovery ranging 98.3-102.3 %. The platforms were successfully applied to quantify SEL in bulk form, Koselugo®capsules, and preliminary applied to human plasma analysis. Eco-friendliness assessment confirmed the adherence of both platforms to green analytical approaches. MW-UV and HPLC-PDA are simple and fast, enabling high throughput analysis, thus, introducing valuable tools for routine use in quality control and clinical laboratories for SEL quantification.

Keywords: selumetinib, UV spectrophotometry, HPLC-PDA, green analytical chemistry, pharmaceutical analysis

Accepted April 12, 2025
Published online April 15, 2025

INTRODUCTION

Neurofibromatosis is a multisystem genetic disorder causing nerve-associated tumors (1). Neurofibromatosis has three types with neurofibromatosis type 1 (NF1) being the most common type, which emerges at birth or in early childhood and affect 1 in 3,500 births (1, 2). It results from a gene mutation in the rat sarcoma (RAS) pathway, impacting neurofibromin protein production essential for cell function (1–3). Mitogen-activated protein kinases 1 and 2 (MEK1/2) are known to regulate the transcription of proteins involved in apoptosis (3). Therefore, the recent development of class-specific MEK1/2 inhibitors has been triggered. These inhibitors can control the problematic cell proliferation that occurs with NF1.

Selumetinib (SEL) is small molecule sold as Koselugo® capsules (AstraZeneca, UK). Its chemical name is: 6-(4-bromo-2-chloroanilino)-7-fluoro-*N*-(2-hydroxyethoxy)-3-methylbenzimidazole-5-carboxamide ($C_{17}H_{15}BrClF_4O_3$, M_r 458 Da) (4); its chemical structure is presented in Fig. 1. On April 10, 2020, SEL has been approved by FDA for the treatment of NF1 and plexiform neurofibromas in paediatric patients (≥2 years) (5, 6). SEL is a non-ATP, competitive and selective MEK1/2 inhibitor, which can effectively blunt the pleiotropic effects of the Ras-Raf-MEK-ERK oncogenic pathway. The inhibition of this pathway reduces cell proliferation and promotes pro-apoptotic signal transduction (7). SEL has shown minimal off-target activity, which contributes to its good safety profile (8). Yet some side effects were reported and in some cases these side effects led to treatment termination, or reduction of the intended dose (9). Linking the drug concentration in its dosage form with its concentrations in

patient's systemic circulation is essential to monitor its efficacy and adverse events. This requires a reliable analytical technique, which can be used in both quality control and clinical laboratory settings.

An extensive literature review revealed that few methods exist for the determination of SEL in capsules (10) and in biological samples (11, 12). These methods are high-performance liquid chromatography with ultraviolet detection (HPLC-UV) for the determination of SEL in capsules (10) and liquid chromatographic methods with tandem mass spectrometry (LC-MS/MS) for the determination of SEL in plasma (11, 12) and whole blood (13). Recently, our laboratory reported a spectrophotometric method for the determination of SEL in bulk and capsules via charge transfer reaction (14). These methods suffer from high cost, complexity, and/or limited throughputs. To address these challenges, the development of improved alternative methodologies was crucial.

Microwell analysis coupled with UV detection (MW-UV), provides high sensitivity and specificity in detecting and quantifying analytes in small sample volumes (15). This technique is particularly useful for high-throughput screening and reduced chemical consumption, and waste production. On the other hand, HPLC-PDA enables precise separation and selective identification of analytes in complex mixtures with high resolution. By promoting procedures efficiency and reducing the environmental footprint of analytical processes, HPLC analysis can align with the principles of green analytical chemistry.

This study introduces, for the first time, the development of two different platforms, MW-UV and HPLC-PDA, for quantitation of SEL in bulk drug, pharmaceutical dosage form (Koselugo® capsules) and human plasma samples. These platforms are characterized with the advantages of high sensitivity, procedures simplicity, environmental sustainability and high throughput.

EXPERIMENTAL

Instrumentation

Multi-mode microplate reader (Spectramax® M5, Molecular Devices, USA) was used. It is equipped with a cuvette port capable of scanning spectra with 1-nm increments and reading up to six wavelengths per scan. Two monochromator optics are installed in the reader making it capable to scan and read a wavelength range of 200-1000 nm. It can accommodate

microplates ranges from 6 to 384 wells in a 4-zone system. The temperature can be controlled up to 50 °C, to maintain the stability of temperature-sensitive assays. Control of the shaking speed (low, medium and high) is achieved *via* an internal shaker. SoftMax® Pro Enterprise software, which complies with FDA 21 CFR Part 11 guidance, was used to control the reader and collect the generated data.

HPLC system (Shimadzu, Japan) equipped with pump (LC-10AD), low pressure flow control valve (FCV-10AL), system controller (SCL-10A), auto-sampler (SIL-30AC), Rheodyne-7725 sample injection valve with 10-µL loop, and a PDA detector (LC-20AD) set at 255 nm was used. A Zorbax Eclipse Plus C18 HPLC column (150 mm length×4.6 mm internal diameter (i.d), 5 µm particle size) was a product of Agilent (USA). A guard column manufactured by Macherey-Nagel GmbH & Co. (Germany) was connected prior to the analytical column. LabSolutions software (version 1.25) was used to control and capture the data.

Microprocessor laboratory pH meter (pH 211, Hanna, Romania), Heidolph vortex mixer (D-91126, Germany), Sigma centrifuge (1-15PK, Merck KGaA, Germany) and Milli-Q water purification system (Millipore Ltd., USA) were used.

Materials

Drug-free adult human plasma samples were sourced from King Khaled University Hospital's Blood Bank in Riyadh, Saudi Arabia. The plasma samples were kept under −20 °C until used. The study was approved by King Saud University Research Ethics Committee (RCE) with Ethics Reference No. KSU-SE-20-51.

A 96-microwell transparent plates were obtained from Corning/Costar Inc. (USA). Finnpipette® single and multi-channel pipettes were obtained from Sigma-Aldrich (USA).

Selumetinib and tozasertib (TOZ) standards were purchased from LC Laboratories (USA); their purities were ≥ 99 %. Koselugo® capsules (AstraZeneca, UK) were purchased from the local market, each capsule labelled to contain 25 mg of SEL.

HPLC grade solvents, surfactants and other chemicals were obtained from Sigma-Aldrich (USA) and Thermo Fischer Scientific (USA).

Standard solutions

Standard stock solutions (2.0 mg mL^{-1}) of SEL and TOZ were prepared in a volumetric flask by accurately weighing and dissolving 20 mg of each standard in 2 mL of dimethyl sulfoxide (DMSO) and completing the volume with acetonitrile. Serial dilution of the SEL stock solution was carried out with H_2O and HPLC mobile phase to produce working solutions in concentration ranges of 15–500 µg mL^{-1} and 0.8–100 µg mL^{-1} for analysis by MW-UV and HPLC-PDA, resp.

Capsule sample solution and analysis

The content of ten Koselugo® capsules were combined and an accurate mass of capsules content equivalent to 20 mg SEL was placed in a 10-mL flask. Two mL of DMSO and 5 mL of acetonitrile were added, then shaken for 30 minutes in ultrasonic bath until completely dissolved. Then, the volume was completed to the mark with acetonitrile, producing solution of expected 2 mg mL^{-1} SEL. The solution was filtered using a 0.4-µm membrane filter. A defined volume of the filtrate was further diluted with H_2O or HPLC mobile phase to create capsule sample solutions with 15–500 and 0.8–100 µg mL^{-1} for analysis by MW-UV and HPLC PDA, resp.

For MW-UV analysis, an accurately measured volume (200 µL) of SEL standard or sample solution (bulk and capsules) was transferred to a well in the 96-microwell plates. The UV absorbance was measured at 255 nm.

For HPLC-PDA, the chromatographic separation was conducted on Zorbax Eclipse Plus C18 HPLC column [150 mm length × 4.6 mm internal diameter (i.d), 5 µm particle size] maintained at 25 ± 2 °C throughout the analysis. The elution was conducted in an isocratic mode with a mobile phase composed of a mixture of ammonium formate buffer solution (0.1 mol L^{-1}) of pH 5 and acetonitrile at a ratio of 65:35 (*V*/*V*) pumped at a flow rate of 1.0 mL min^{-1}. Aliquots (10 µL) of the standards and capsule samples were injected into the HPLC system by the autosampler. The elution of the compounds was monitored by the PDA detector (set at 255 nm). The relation between the peak area ratio of SEL to TOZ peaks and the SEL concentration was used as the basis for the quantification.

Plasma samples and analysis

From the human plasma sample, 1 mL was spiked with SEL standard solution, mixed with the same volume of methanol, vortexed and centrifuged at 13,000 rpm for 10 min. The supernatants were aspirated and passed through 0.2-µm Millipore filter syringes. The filtrates were spiked with TOZ (internal standard) and diluted with HPLC mobile phase to give SEL

concentrations in the range of 0.8–100 μg mL^{-1} and a fixed concentration of TOZ (5 μg mL^{-1}). HPLC analysis of the plasma samples was done following previously mentioned analysis method for capsules.

Validation of MW-UV and HPLC-PDA

Validation of the proposed MW-UV and HPLC-PDA platforms was done according to the International Council on Harmonisation (ICH) guidelines for the validation of analytical procedures (16) and bioanalytical method validation and study sample analysis M10 (17). All calculations were in this study were based on calibration using standard drug solutions (model standards).

Linearity and sensitivity. – To assess the linearity range, series of SEL concentrations of standard solutions were analyzed. These concentration ranges were 5–800 and 0.5–200 μg mL^{-1} for MW-UV and HPLC-PDA, resp. These solutions were prepared from the stock solution by its dilution in water or the mobile phase for analysis by MW-UV or HPLC-PDA, resp. Linear regression equations and their determination coefficients (R^2) were calculated from three independent calibration curves of at least five concentration levels.

The limit of detection (*LOD*) and limit of quantification (*LOQ*) were used to evaluate the methods sensitivity, following the formula:

$$LOD \text{ or } LOQ = \times \mathrm{SDa}/b$$

where × is 3.3 for *LOD* and 10 for *LOQ*, SDa is the standard deviation of the calibration line intercept, while *b* is the calibration line slope.

Precision and accuracy. – Five SEL concentration levels, covering the entire linear working ranges of the platforms, were used. Three replicates of each concentration point in the ranges of 25–400 and 10–80 μg mL^{-1} for MW-UV and HPLC-PDA, resp., were analysed to determine intra-assay precision and accuracy.

Assessment of the inter-assay was done over three consecutive days by analysing six replicate samples of each concentration point of the five concentration points in the same ranges by two analysts.

Percentage of recovery was derived from comparing the measured concentrations to the specified concentrations.

Effect of plasma matrix. – To assess the effect of plasma matrix, four samples were analyzed under different conditions: a SEL-free sample (blank plasma without SEL and without IS), blank plasma spiked with IS (5 µg mL^{-1}), blank plasma spiked with both SEL at *LOQ* concentration (3.5 µg mL^{-1}) and IS at a concentration of 5 µg mL^{-1}, and blank plasma spiked with both SEL at a concentration of 10 µg mL^{-1} and IS at a concentration of 5 µg mL^{-1}. The chromatograms were investigated for appearance of any interfering peaks at the retention times of both SEL and IS. Additionally, varying SEL concentrations (20, 40, 60 and 80 µg mL^{-1}) were spiked in plasma samples, and analyzed by the proposed HPLC-PDA method. The mean recovery for each concentration level was calculated.

RESULTS AND DISCUSSION

Selection of detection wavelength

SEL chemical structure features chromophore functional groups due to the conjugated systems (Fig. 1). Therefore, the compound is expected to absorb light within UV wavelength. This assertion was confirmed through its UV absorption spectrum (Fig. 1), illustrating SEL's pronounced UV light absorption within the 200 – 400 nm range, with a prominent absorption peak at 255 nm. This discovery prompted the utilisation of SEL's absorption characteristics in the development of MW-UV and HPLC-PDA platforms for the analysis of SEL in capsules and plasma samples.

Development of MW-UV

To ensure high absorbance intensity, some factors were optimized like microwell plates, solvents, surfactants, acidity, *etc*. Table 1S summarizes the optimized values of the variables.

Solvents. - The solvents tested were water, methanol, ether, acetone, propanol, pentanol, acetonitrile, dimethylformamide, chloroform and hexane. The absorption spectra of SEL solutions in these solvents are given in Fig. 1S, and the absorption values at the maximum absorption peaks are given in Fig. 2a. The highest UV absorption intensity was attained in acetone and dimethylformamide; nevertheless, both solvents possess UV cutoff wavelengths at 330 and 270 nm, resp. (18), which overlap with the absorption spectrum of SEL. This overlap led to their exclusion from further evaluation. Hexane exhibited the least absorbance, while other solvents, including water, displayed comparable absorption intensities. Water was favoured as the preferred solvent for subsequent experiments.

Surfactants. - The addition of surfactants, owing to their amphiphilic properties, can induce micelle formation, thereby enhancing the UV absorption intensity of the solute (19, 20). In this study, various types of surfactants-such as anionic (CMC - carboxymethyl cellulose, SLS - sodium lauryl sulfate, SD - sodium dodecyl sulfate), cationic (cetrimide), and non-ionic (Tween 20, Tween 80, chromophor EL) were investigated for their impact on the UV absorption of SEL. Results indicated a slight decrease in SEL's UV absorption with the addition of SLS, SDS and Tween 20, compared to scenarios without surfactants (Fig. 2b). However, most surfactants either maintained similar absorption levels or slightly increased SEL absorption compared to its solution in water. While surfactants are known to enhance the solubility of hydrophobic drugs like SEL by forming micellar systems, the observed UV absorptivity did not significantly increase with surfactant presence in this study. Previous reports suggest that while a single or combined surfactants can enhance solubility and absorptivity of hydrophobic drugs (21, 22), however, the observed results here did not show significant increase in the UV absorptivity of SEL. Accordingly, use of surfactant was excluded in the subsequent experiments.

Acidity. - To investigate the impact of pH on the absorbance spectrum, a series of SEL solutions were prepared in Britton Robinson buffer of varying pH values (pH 3–12) (Fig. 2c). The results indicated that the absorption intensity of SEL was not affected by pH change, except for a slight increase which occurred at pH 9. To elucidate this outcome further analysis using MarvinSketch (ChemAxon, Budapest, Hungary) was carried out (23, 24) as detailed in the supplementary material (Fig. 2S).

Sample solution volume. - The optimal volume of SEL sample solution (250 µg mL^{-1}) for analysis was determined by measuring the UV absorbance intensity of 50, 100, 150, 200, and 250 µL per well in a 96-well plate. Precision was improved with increasing volume up to 200 µL per well (RSD 0.8 %). Beyond this point a lower precision (RSD 3.8 %) was observed (Fig. 3S).

Validation of MW-UV

Linearity and sensitivity. – MW-UV linear relationships were evident between SEL concentration and signals in the range of 15–500 µg mL^{-1} with a coefficient of determination (R^2) of 0.999. The calibration line and its corresponding linear fitting equation is given in Fig. 4S.

LOD and *LOQ* found to be 5.1 and 15.3 µg mL^{-1}, resp. Table I provides a summary of

the calibration parameters for SEL quantification using MW-UV platform.

Precision and accuracy. – The intra- and inter-day RSDs ranged from 0.6 to 1.5 % and 1.2 to 1.8 %, resp.

Accuracy evaluation was conducted at the same concentration levels used for precision assessment. Accuracy evidenced by recovery values ranged 98.3–102.3 %. The precision and accuracy profile in terms of RSD and recovery are summarized in Table III.

As seen in Table IV, representing the platform intermediate precision, variations attributable to the analysts did not surpass 1.4 % for RSD and 101.2 % for recovery. The day-to-day RSD did not exceed 2.4 %; recovery values ranged between 99.8 and 101.2 %.

Throughputs of MW-UV

Microwell-based techniques represent efficient tools for conducting high-throughput analyses, enabling the concurrent processing of numerous samples in a cost-effective manner. The platform exhibits rapid samples processing, handling multiple samples simultaneously in a batch format. A single analyst can manage up to 6 plates as a batch (equivalent to 576 samples) within approximately 30 min (*i.e*., 1152 samples per hour), encompassing tasks from sample preparation and dispensing through to data processing and result generation. Furthermore, the throughput of platform can be easily scalable and amenable to automation by utilising plates with a higher well count (such as 384- and 1536-well plates) and robotic systems. This scalability and automation potential not only boost high-throughput capacity but also enhance efficiency, minimize errors, and streamline operations, thereby saving valuable time and effort in the laboratory.

Development of HPLC-PDA

Internal standard. - In the selection of the most suitable IS, drugs belonging to the tyrosine kinase inhibitors class, namely, tozasertib, afatinib, linifanib and pelitinib, were selected for investigation. The chemical structures of these drugs are depicted in Fig. 5S. Examination of the absorption spectra of these drugs revealed a spectral overlap with SEL (as illustrated in Fig. 6S), allowing their detection at the same wavelength of 255 nm, designated for SEL. Initial chromatographic trials demonstrated that TOZ could be effectively separated from SEL under the preliminary chromatographic conditions specified for SEL. Consequently, TOZ was chosen as the IS for subsequent investigations.

Optimization of the chromatographic conditions. - To optimize the chromatographic conditions for efficient separation and detection of SEL and TOZ within a short time frame, various system parameters such as the mobile phase composition, column, and flow rate were systematically investigated. All experimental procedures were conducted at room temperature. Initially, the following conditions were employed: a C18 reversed-phase column (150 mm length × 4.6 mm inner diameter, 5 μm particle diameter), isocratic elution, using a mobile phase consisting of a mixture of ammonium formate buffer solution (0.1 %) adjusted to pH 3 and acetonitrile at a ratio of 40:60 (*V*/*V*), and a flow rate of 1 mL min^{-1}. Under these conditions, both SEL and TOZ were separated in a short period (<7 min), but the peak resolution was not sufficient. This proximity in retention times can be attributed to the lipophilic nature of both compounds, with the high content of acetonitrile in the mobile phase leading to rapid elution and resulting in peak overlap. To improve the separation while maintaining a short analysis time, the pH of buffer was adjusted to pH 5, while using the same mobile phase ratio. This adjustment resulted in a slight enhancement of TOZ peak separation, while preserving the retention time of SEL and the efficiency of the rapid analysis. Furthermore, it was noted that alterations in pH had a minimal impact on the chromatographic behaviour of SEL, in contrast to TOZ, which exhibited a notable sensitivity to pH variations. To explain this differential behaviour, computational simulations were executed to ascertain the protonation states of both SEL and TOZ across a range of pH levels using the MarvinSketch software (ChemAxon, Budapest, Hungary) (23). The computational analysis delineated the potential protonated states of both SEL and TOZ, along with their corresponding distribution of microspecies in relation to pH, as depicted in Figs. 2S and 7S. The subtle electronic disparities between these states resulted in minimal impact on its chromatographic behaviour when transitioning from pH 1 to 3; conversely, TOZ varying protonated states account for the sensitivity of TOZ alterations in the mobile phase pH from 3 to 5.

Further adjustments to the mobile phase composition were made by reducing the acetonitrile percentage (ammonium acetate: acetonitrile ratio of 65:35, *V*/*V*). This modification led to improved separation and retention times for both SEL and TOZ (9.1 and 5.7 min, resp.) with an acceptable resolution. In order to obtain a higher resolution, the ratio of ammonium acetate to acetonitrile to 70:30 (*V*/*V*) was adjusted. While this adjustment achieved a higher peak resolution, it also resulted in extended retention times for SEL and TOZ (16.5 and 9.2 min, resp.), impacting the overall analysis time.

The mobile phase ratio of 65:35 (*V*/*V*) ammonium acetate to acetonitrile was determined to be optimal as it yielded a resolution greater than 1 between SEL and TOZ, symmetric peaks for both TOZ and SEL across different concentrations (as depicted in Figs. 3a and 3b) and maintained a total analysis time within an acceptable range (<10 min). To assess the suitability of the chromatographic system under these selected conditions, various key parameters including the capacity factor, separation factor, resolution factor, and peak symmetry were evaluated. The results of these evaluations are summarized in Table IV.

A summary of all mobile phase optimization efforts for the separation of SEL and TOZ is presented in Table 2S.

Validation of HPLC-PDA

Linearity and sensitivity. - HPLC-PDA calibration curve used to quantify SEL is presented in Fig. 8S. Linear relationship was evident between SEL concentration and signals in the range of 0.8–100 µg mL^{-1} and the R^2 was calculated as 0.9996.

The *LOD* and *LOQ* were determined to be 1.1 and 3.5 µg mL^{-1}, resp. Table V provides a summary of the calibration parameters for SEL quantification using the HPLC-PDA.

Precision and accuracy. – Intra- and inter-assays assessment was conducted across SEL concentrations ranging from 10 to 80 µg mL^{-1}. The intra-day RSD varied from 0.6 to 1.5 %, while inter-day precision ranged from 1.1 to 1.8 %.

Recovery fell between 98.6 and 101.2 % (Table VI).

HPLC-PDA intermediate precision assessment details are given in Table VII. The highest analysts-related and analysis day RSDs were 2.4 %.

Throughputs of HPLC-PDA

The throughput of HPLC-PDA platform was evaluated using a 15-minute runtime as a benchmark. With this runtime, the platform can process up to 4 samples per hour. Adjusting HPLC conditions, such as increasing the flow rate, has the potential to improve throughput; however, it must be done carefully not to compromise the separation of the analyte.

Applications of MW-UV and HPLC-PDA

Analysis of bulk drug and capsules. – The validated MW-UV and HPLC-PDA platforms were employed to determine the concentration in bulk form and Koselugo® capsules. The mean

recovery, obtained by MW-UV and HPLC-PDA were 100.1 ± 1.1 % and 99.8 ± 1.4 % for analysis of bulk form and Koselugo® capsules, resp. (Table VIII).

For HPLC-PDA, the chromatograms obtained from analysis of standard SEL solution and Koselugo® capsules solution are shown in Fig. 4 and the original chromatograms are in Fig. 9S. The chromatogram of Koselugo® capsules does not show any interfering peaks at the retention times of both SEL and IS, demonstrating the selective determination of SEL in the capsules. The obtained mean analytical recoveries (± RSD) were 100.2 ± 1.7 % and 100.1 ± 2.1 % for the bulk form and Koselugo® capsules, resp. (Table VIII).

To assess reliability of new platforms comparison was performed *versus* published method (10), through accuracy and precision (Table VIII). Results were statistically compared with those of the proposed platforms using *t*-test and *F*-test at 95 % confidence interval. All the calculated *t*- and *F*-values were lower than the tabulated ones, revealing that there were no significant differences in the accuracy and precision of the proposed MW-UV and HPLC-PDA compared with the reference method.

Preliminary research on analysis of plasma samples

Before utilising the HPLC-PDA platform for analysing plasma samples, the effect of plasma matrix on the performance of the platform was evaluated by analysing blank SEL-free human plasma samples. Fig. 5 (originals in Fig. 10S) illustrates representative chromatograms of plasma under four distinct conditions: a SEL-free sample (blank plasma), blanka plasma spiked with IS at a concentration of 5 μg mL^{-1}, blank plasma spiked with both SEL at the *LOQ* concentration (3.5 μg mL^{-1}) and IS at a concentration of 5 μg mL^{-1}, and blank plasma spiked with both SEL at a concentration of 10 μg mL^{-1} and IS at a concentration of 5 μg mL^{-1}. As depicted in Fig. 5, no noticeable interfering peaks were detected at the respective retention times of both SEL and IS. Furthermore, there was no evidence of carryover for either SEL or IS in plasma samples, as indicated by the absence of any interfering peaks following the injection of plasma samples containing the *LOQ*.

In a subsequent series of experiments, varying SEL concentrations (20, 40, 60 and 80 μg mL^{-1}) were spiked into plasma samples, and analysed by the proposed HPLC-PDA method. The mean recovery was 100.1 ± 2.1 %, demonstrating the accuracy and precision of the platform for analysis of plasma samples containing SEL.

It is important to note the current HPLC-PDA method's linearity range and *LOQ* are indeed higher than the stated C_{max} indicating that current experiments of plasma analysis are of

preliminary nature at the moment. Currently, we are actively considering modifications to the method to enhance its sensitivity. The approaches include sample preparation protocol and methodology: (*i*) Analyte concentration techniques implementing liquid-liquid extraction or solid-phase extraction to concentrate the analyte, thereby lowering the *LOQ* and extending the linearity range to cover the expected therapeutic concentrations. Preliminary promising results were obtained, demonstrating the enhancement of method's sensitivity by 10 folds; (*ii*) Advanced detection methods exploring the use of more sensitive detection techniques, such as tandem mass spectrometry with optimized ionization conditions, to enhance the method's sensitivity; (*iii*) Microsampling approaches incorporating microsampling techniques to improve the detection of low analyte concentrations.

Greenness of MW-UV and HPLC-PDA

The green analytical chemistry (GAC) approach aims to reduce the harmful impacts of chemicals, materials, and techniques used in chemical analysis workflows, as well as the resultant waste (25). To assess the greenness of both MW-UV and HPLC-PDA, three tools were employed. These tools were the Analytical Eco-Scale (AES) (26), Green Analytical Procedure Index (GAPI) (27), and Analytical Greenness (AGREE) (28). All three tools are metric tools and capable of offering dependable evaluations of the eco-friendliness of the proposed platforms by conducting a systematic assessment across multiple parameters. By following the procedures outlined in the respective references, the results are presented in Table IX for AES, Fig. 6a for GAPI and Fig. 6b for AGREE.

As for AES, it evaluates the eco-friendliness based on penalty points (PPs) of four major parameters (Table IX). Evaluation of MW-UV aligned 4 PPs with solvent (1 and 3 PP with solvent amount and hazards, resp.), and 4 PPs with waste (1 and 3 PPs for waste production and treatment, resp.). The total PPs are 8, resulting in eco-scale score of 92 (100-8) PPs. The HPLC-PDA assessment resulted in higher total PPs of 18, and lower eco-scale score of 82 (100-18). Both scores represent high level (>75) of greenness of the platforms.

In the GAPI pictograms for both MW-UV and HPLC-PDA, parameters 1 and 15 (related to sample collection/preparation and waste treatment, resp.) were highlighted in red. This red highlighting was applied because sample collection/preparation was conducted offline, and waste treatment was lacking for both platforms. Parameter 5 (method type) was marked in yellow for both MW-UV and HPLC-PDA since they are both direct quantitative methods. Parameter 9 (reagent and solvent amount) was assigned as green in MW-UV because water

was used as a solvent; however, the parameter was yellow in HPLC-PDA because the platform used acetonitrile and ammonium formate buffer in the mobile phase. In conclusion, the overall greenness scores, expressed as percentages of green parameters/total parameters, of MW-UV and HPLC-PDA are 11/15 (73.3 %) and 8/15 (53.3 %), resp.

The AGREE report sheet, showing the score and weight of each parameter is given in Fig. 11S. In the AGREE tool, parameter 3 (analytical device positioning) in both MW-UV and HPLC-PDA was highlighted in red because the analysis was conducted offline using a microplate reader and an HPLC system. Parameter 1 (sampling procedure) in MW-UV was marked in orange, while parameters 7 (amount of waste) and 8 (analysis throughput) in HPLC-PDA were also denoted in orange. Furthermore, parameter 1 in HPLC-PDA was indicated in yellow due to the manual handling of samples. Following the tool recommendations and the various colour assignments (ranging from green to red), MW-UV scored a total of 0.78, and HPLC-PDA scored 0.68. This indicates that both methods are environmentally friendly, with MW-UV exhibiting a higher level of greenness compared to HPLC-PDA.

CONCLUSIONS

Considering, the key advantages of the native UV light absorption-assisted analytical techniques, the approach was attempted in this study to develop MW-UV and HPLC-PDA platforms for SEL analysis. Comparative analysis of both platforms revealed a wider linearity range of MW-UV (15 – 500 µg mL^{-1}) than HPLC-PDA (0.8 – 100 µg mL^{-1}). The HPLC-PDA showed lower limiting values (*LOD* 1.1 µg mL^{-1}) than MW-UV (*LOD* 5.1 µg mL^{-1}). The overall recovery of the MW-UV ranged from 98.3 to 102.3 %, and from 98.6 to 101.2 % for HPC-PDA. Similarly, the overall RSD was 0.6-1.8 % for the two methods. Both platforms showed a satisfactory eco- friendliness profile with MW-UV possessing a better profile in the three GAC tools applied. The comparison between MW-UV and HPLC-PDA platforms reveals that MW-UV offers a wider linear range, higher throughput using 96-well plates, and greater eco-friendliness, while HPLC-PDA is more sensitive, though both methods are comparable in accuracy and precision, with MW-UV benefiting from concurrent sample preparation and HPLC-PDA from system consistency. In conclusion, both methodologies can be used for the SEL quantification in dosage forms (Koselugo® capsules) with high reliability. The choice between MW-UV and HPLC-PDA hinges on instrument availability, the number of samples to be analysed, and the SEL concentration levels of the samples.

While, the HPLC-PDA platform demonstrated promising results, its applicability in clinical settings need additional enhancement in terms of sensitivity and revalidation for analysis of biological specimens. These studies will be undertaken in future work to ensure the method's suitability for clinical applications.

Acknowledgments. – The authors extend their appreciation to the Researchers Supporting Project number (RSP2025R215), King Saud University, Riyadh, Saudi Arabia, for funding this work.

Conflict of interest. - The authors declare that they have no known competing financial interests or personal relationships that could have appeared to influence the work reported in this paper.

Data availability. - All data generated or analysed during this study are included in this published article and in the supplementary material.

Authors contribution. - Sara Alrubia: Methodology, Investigation, Data curation, Formal analysis, Validation, Writing – original draft. Wafa A. AlShehri: Conceptualization, Investigation, Data curation, Formal analysis, Validation, Writing – original draft. Nourah Z. Alzoman: Methodology, Visualization, Funding acquisition, Writing – review & editing. Ibrahim A. Darwish: Methodology, Supervision, Project administration, Writing – review & editing.

Financing. - The work was funded by the Researchers Supporting Project number (RSP2024R215), King Saud University, Riyadh, Saudi Arabia, for funding this work.

ORCIDs. - Ibrahim A Darwish (0000-0003-3821-623X), Nourah Alzoman (0000-0003-4471-2344), Sarah Alrubia (0000-0003-1892-2452).

REFERENCES

1. D. H. Gutmann, R. E. Ferner, R. H. Listernick, B. R. Korf, P. L. Wolters and K. J. Johnson, Neurofibromatosis type 1, *Nat. Rev. Dis. Primer* **3** (2017) 17004; https://doi.org/10.1038/nrdp.2017.4
2. A. S. Michaels, *Neurofibromatosis: Causes, Tests and Treatment Options* (2nd ed.). CreateSpace Independent Publishing Platform, Scotts Valley (CA, USA) 2014.
3. I. Solares, D. Viñal, M. Morales-Conejo, N. Rodriguez-Salas and J. Feliu, Novel molecular targeted therapies for patients with neurofibromatosis type 1 with inoperable plexiform neurofibromas: a comprehensive review, *ESMO Open* **6**(4) (2021) Article ID 100223; https://doi.org/10.1016/j.esmoop.2021.100223

4. R. Roskoski, Properties of FDA-approved small molecule protein kinase inhibitors: A 2021 update, *Pharmacol. Res.* **165** (2021) Article ID 105463; https://doi.org/10.1016/j.phrs.2021.105463

5. D. Casey, S. Demko, A. Sinha, P. S. Mishra-Kalyani, Y.-li Shen, S. Khasar, M. A. Goheer, W. S. Helms, L. Pan, Y. Xu, J. Fan, R. Leong, J. Liu, Y. Yang, K. Windsor, M. Ou, O. Stephens, B. Oh, G. H. Reaman, A. Nair, S. S. Shord, V. Bhatnagar, S. R. Daniels, S. Sickafuse, K. B. Goldberg, M. R. Theoret, R. Pazdur and H. Sing, FDA approval summary: Selumetinib for plexiform neurofibroma, *Clin. Cancer Res.* **27**(15) (2021) 4142–4146; https://doi.org/10.1158/1078-0432.CCR-20-5032

6. U.S. Food & Drug Administration, *FDA Approves Selumetinib for Neurofibromatosis Type 1 with Symptomatic, Inoperable Plexiform Neurofibromas*, US-FDA, Silver Spring (MD, USA), April 13, 2020; https://www.fda.gov/drugs/resources-information-approved-drugs/fda-approves-selumetinib-neurofibromatosis-type-1-symptomatic-inoperable-plexiform-neurofibromas; last access date September 22, 2024

7. S. V. Holt, A. Logié, R. Odedra, A. Heier, S. P. Heaton, D. Alferez, B. R. Davies, R. W. Wilkinson and P. D. Smith, The MEK1/2 inhibitor, selumetinib (AZD6244; ARRY-142886), enhances anti-tumour efficacy when combined with conventional chemotherapeutic agents in human tumour xenograft models, *Br. J. Cancer* **106** (2012) 858–866; https://doi.org/10.1038/bjc.2012.8

8. C. Li, Z. Chen, H. Yang, F. Luo, L. Chen, H. Cai, Y. Li, G. You, D. Long, S. Li, Q. Zhang and L. Rao, Selumetinib, an oral anti-neoplastic drug, may attenuate cardiac hypertrophy via targeting the ERK pathway, *PloS One* **11** (2016) e0159079; https://doi.org/10.1371/journal.pone.0159079

9. FDA - Center for Drug Evaluation and Research, *NDA Multi-disciplinary Review and Evaluation NDA 213756 Koselugo (selumetinib)*, Version July 24, 2019, US FDA-CDER, Silver Spring (MD, USA), February 2020; https://www.accessdata.fda.gov/drugsatfda_docs/nda/2020/213756Orig1s000MultidisciplineR.pdf; last access date August 3, 2024

10. K. K. Saindane, H. Talapadatur, V. K. Munipalli, R. M. Singh, B. Fegade and V. Bhaskar, Stability indicating RP-HPLC method for the estimation of selumetinib in capsule dosage form, *Int. J. Pharm. Sci. Rev. Res.* **74** (2022) 166–174; https://doi.org/10.47583/ijpsrr.2022.v74i02.026

11. P. Severin, C. Bailey, M. Chen, A. Fisher and V. Holmes, Determination of selumetinib, N-desmethyl selumetinib and selumetinib amide in human biological samples by LC-MS/MS, *Bioanalysis* **8** (2016) 1919–1936; https://doi.org/10.4155/bio-2016-0082

12. J. Li, Z. Zhang, M. Yan, S. Yang, Y. Song and J. Dong, Determination of selumetinib in rat plasma by UPLC-MS/MS and application to a pharmacokinetic study, *Lat. Am. J. Pharm.* **39** (2020) 237–342.

13. R. R. Voggu, T. S. Brus, C. T. Barksdale, P. Severin, P. Hansen, R. Chudnovskiy, E. Thomas and C. Bailey, Novel LC-MS/MS method for the determination of selumetinib (AZD6244) in whole

blood collected with volumetric absorptive microsampling, *Bioanalysis* **12** (2020) 883–892; https://doi.org/10.4155/bio-2020-0062

14. S. Alrubia, W.A. AlShehri, A.A. Radwan, N.Z. Alzoman and I.A. Darwish, Spectrophotometric and computational characterization of charge transfer complex of selumetinib with 2,3-dichloro-5,6-dicyano-1,4-benzoquinone and its utilization in developing an innovative green and high throughput microwell assay for analysis of bulk form and pharmaceutical formulation, *BMC Chemistry* **19** (2025) Article ID 27 (17 pages); https://doi.org/10.1186/s13065-024-01353-6
15. I. A. Darwish and N. Z. Alzoman, Development of green and high throughput microplate reader-assisted universal microwell spectrophotometric assay for direct determination of tyrosine kinase inhibitors in their pharmaceutical formulations irrespective the diversity of their chemical structures, *Molecules* **28**(10) (2023) Article ID 4049 (19 pages);
16. International Conference for Harmonisation (ICH), *Harmonised Guideline Q2 (R1) Validation of Analytical Procedures: Text and Methodology*, Geneva, Dec 2023; Retrieved from https://database.ich.org/sites/default/files/ICH_Q2-R2_Document_Step2_Guideline_2022_0324.pdf; last access March 18, 2025
17. International Conference for Harmonisation (ICH)/EMA, H*armonised Guideline (M10) Bioanalytical Method Validation and Study Sample Analysis*-Step 4, Geneva, May 2022; https://database.ich.org/sites/default/files/M10_Guideline_Step4_2022_0524.pdf; last access March 18, 2025
18. Waters, Wavelength cutoffs for common solvents; https://help.waters.com/help/en/product-support/alliance-is-system-support/715008450/6BCFA49.html; last access March 18, 2025
19. A. Yusaf, M. Usman, A. Mansha, M. Siddiq, Z. Amjad, S. Irshad and H. Sultana, Self-organised surfactant assemblies as nanostructured dye carriers: a mixed micellar comparative approach for enhanced dye solubilisation, *Int. J. Environ. Anal. Chem.* **104** (2024) 2352–2363; https://doi.org/10.1080/03067319.2022.2060747
20. A. A. Rana, A. Yusaf, S. Shahid, M. Usman, M. Ahmad, S. Aslam, S. A. Al-Hussain and M. E. A. Zaki, Unveiling the role of nonionic surfactants in enhancing cefotaxime drug solubility: a uv-visible spectroscopic investigation in single and mixed micellar formulations, *Pharmaceuticals* **16**(12) (2023) Article ID 1663; https://doi.org/10.3390/ph16121663
21. P. Patel, E. Howgate, P. Martin, D. J. Carlile, L. Aarons and D. Zhou, Population pharmacokinetics of the MEK inhibitor selumetinib and its active N-desmethyl metabolite: data from 10 phase I trials, *Br. J. Clin. Pharmacol.* **84** (2018) 52–63; https://doi.org/10.1111/bcp.13404
22. F. Shakeel, S. Alshehri, M. A. Ibrahim, M. Altamimi, N. Haq, E. M. Elzayat and G. A. Shazly, Solubilization and thermodynamic properties of simvastatin in various micellar solutions of different non-ionic surfactants: Computational modeling and solubilization capacity, *PLoS ONE* **16** (2021) e0249485; https://doi.org/10.1371/journal.pone.0249485

23. ChemAxon. MarvinSketch Version 23.12., (Chemaxon Ltd., Budapest, Hungary); Retrieved from https://chemaxon.com/marvin; last access March 18, 2025
24. D. Malyshev, R. Öberg, L. Landström, and P. O. Andersson, T. Dahlberg, M. Andersson. pH-induced changes in Raman, UV–vis absorbance, and fluorescence spectra of dipicolinic acid (DPA), *Spectrochim. Acta A* **271** (2022) Article ID 120869 (8 pages); https://doi.org/10.1016/j.saa.2022.120869
25. S. Armenta, S. Garrigues and M. de la Guardia, Green analytical chemistry, *TrAC Trends Anal. Chem.* **27** (2008) 497–511; https://doi.org/10.1016/j.trac.2008.05.003
26. A. Gałuszka, Z. M. Migaszewski, P. Konieczka and J. Namieśnik, Analytical Eco-Scale for assessing the greenness of analytical procedures, *TrAC Trends Anal. Chem.* **37** (2012) 61–72; https://doi.org/10.1016/j.trac.2012.03.013
27. J. Płotka-Wasylka, A new tool for the evaluation of the analytical procedure: Green analytical procedure index, *Talanta* **181** (2018) 204–209; https://doi.org/10.1016/j.talanta.2018.01.013
28. F. Pena-Pereira, W. Wojnowski and M. Tobiszewski, AGREE—Analytical GREEnness Metric approach and software, *Anal. Chem.* **92** (2020) 10076–10082; https://doi.org/10.1021/acs.analchem.0c01887

Table I. Calibration parameters for the determination of SEL by MW-UV

Parameter	Value[a]
Linear range (µg mL^{-1})	15 – 500
Intercept (a)	0.0325
Standard deviation of intercept (SD_a)	0.0066
Slope (b)	0.0043
Standard deviation of slope (SD_b)	0.0015
Determination coefficient (R^2)	0.999
Residual sum of the squares	0.0039
Limit of detection (*LOD*, µg mL^{-1})	5.1
Limit of quantitation (*LOQ*, µg mL^{-1})	15.3

[a] Mean of three determinations.

Table II. Accuracy of MW-UV for the determination of SEL at different concentration levels

SEL concentration (µg mL^{-1})	Recovery (% ± RSD)	
	Intra–assay, *n = 3*	Inter–assay, *n = 6*
25	99.5 ± 1.1	101.2 ± 1.4
100	100.6 ± 0.8	98.3 ± 1.2
200	101.2 ± 0.6	99.4 ± 1.4
300	102.3 ± 1.5	99.8 ± 1.8
400	98.8 ± 1.2	102.2 ± 1.6

Table III. Intermediate precision of MW-UV for the determination of SEL

Parameter	Recovery (%) [a]	Precision (RSD, %)
Analyst to-analyst		
Analyst-1	101.2	1.4
Analyst-2	100.4	1.2
Day-to-day		
Day-1	99.8 4	2.4
Day-2	100.5	2.1
Day-3	101.2	1.4

[a] Mean of three determinations.

Table IV. Chromatographic system suitability parameters of the determination of SEL by HPLC-PDA

Parameter	Value
Retention time for SEL (min) [a]	9.091 ± 0.201
Retention time of TOZ (min) [a]	5.686 ± 0.101
Capacity factor (*k`*)	2.357
Separation factor (α)	1.159
Resolution factor (R_s)	5.259
Peak asymmetry factor	1.159
Number of theoretical plates (plate/meter) (*N*)	10842

[a] *n*=3.

Table V. Calibration parameters for the determination of SEL by HPLC-PDA

Parameter	Value [a]
Linear range (μg mL^{-1})	0.8 – 100
Intercept (a)	0.0965
Standard deviation of intercept (SD_a)	0.0569
Slope (b)	0.1646
Standard deviation of slope (SD_b)	0.0265
Determination coefficient (R^2)	0.9996
Residual sum of the squares	0.0975
Limit of detection (*LOD*, μg mL^{-1})	1.1
Limit of quantitation (*LOQ*, μg mL^{-1})	3.5

[a] Mean of three determinations.

Table VI. Accuracy of HPLC-PDA for the determination of SEL at different concentration levels

SEL concentration (μg mL^{-1})	Recovery (% ± RSD)	
	Intra–assay, *n = 3*	Inter–assay, *n = 6*
10	99.6 ± 1.2	100.4 ± 1.5
20	101.2 ± 0.6	99.5 ± 1.1
40	100.4 ± 1.1	98.6 ± 1.4
60	99.3 ± 1.2	101.2 ± 1.6
80	98.6 ± 1.5	100.4 ± 1.8

Table VII. Intermediate precision of HPLC-PDA for the determination of SEL

Parameter	Recovery (%) [a]	Precision (RSD, %)
Analyst to-analyst		
Analyst-1	100.8	1.6
Analyst-2	99.6	2.4
Day-to-day		
Day-1	97.6	2.1
Day-2	99.8	2.4
Day-3	102.1	1.8

[a] Mean of three determinations.

Table VIII. Analysis of SEL in bulk and Koselugo® capsule by MW-UV and HPLC-PDA

Nominal concentration (μg mL^{-1})	SEL bulk form			Koselugo® capsule		
	Found concentration (μg mL^{-1}) [a]		Recovery (%)[a]	Found concentration (μg mL^{-1}) [a]		Recovery (%)[a]
			MW-UV			
50	50.4		100.8 ± 1.2	49.4		98.8 ± 1.4
100	98.8		98.8 ± 1.4	101.2		101.2 ± 0.8
200	202.5		101.3 ± 1.6	186.8		98.4 ± 1.6
400	398.5		99.6 ± 1.8	402.8		100.7 ± 1.4
		Mean	100.1 (98.6)[b]		Mean	99.8 (101.2)[b]
		RSD	1.1 (1.5)[b]		RSD	1.4 (1.8)[b]
		t-value	1.396 (3.182) [c]		*t*-value	1.063 (3.182) [c]
		F-value	1.860 (9.28) [c]		*F*-value	1.654 (9.28) [c]
			HPLC-PDA			
20	19.9		99.5	20.3		101.5
40	40.5		101.3	39.4		98.5
60	58.9		98.2	61.4		102.3
80	81.5		101.9	78.6		98.3
		Mean	100.2 (98.6[b])		Mean	100.1 (101.2[b])
		RSD	1.7 (1.5[b])		RSD	2.1 (1.8[b])
		t-value	1.222 (2.776[c])		*t*-value	1.007 (2.776[c])
		F-value	1.284 (19.00[c])		*F*-value	1.361 (19.00[c])

[a] Mean of three determinations.

[b] Values in parentheses are obtained by the literature method (ref. 10).

[c] Values in parentheses are the tabulated *t*- and *F*-values at the corresponding degrees of freedom (df) at confidence level of 95 %; three independent values.

Table IX. Analytical eco-scale for assessing the greenness of MW-UV and HPLC-PDA platforms for determination of SEL

Eco-scale score parameters		Penalty points (PPs)	
		MW-UV	HPLC-PDA
Solvent/reagent			
Amount: acetonitrile (<1 mL per sample)		1	6
Hazards: acetonitrile		3	3
Instrument: Energy used (kWh per sample)			
Microplate reader		0	1
Occupational hazardous			
Analytical process hermetic		0	0
Emission of vapours and gases to the air		0	0
Waste			
Production (<1 mL per sample)		1	5
Treatment (No treatment involved)		3	3
	Total PPs	8	18
	Eco-scale score	92	82

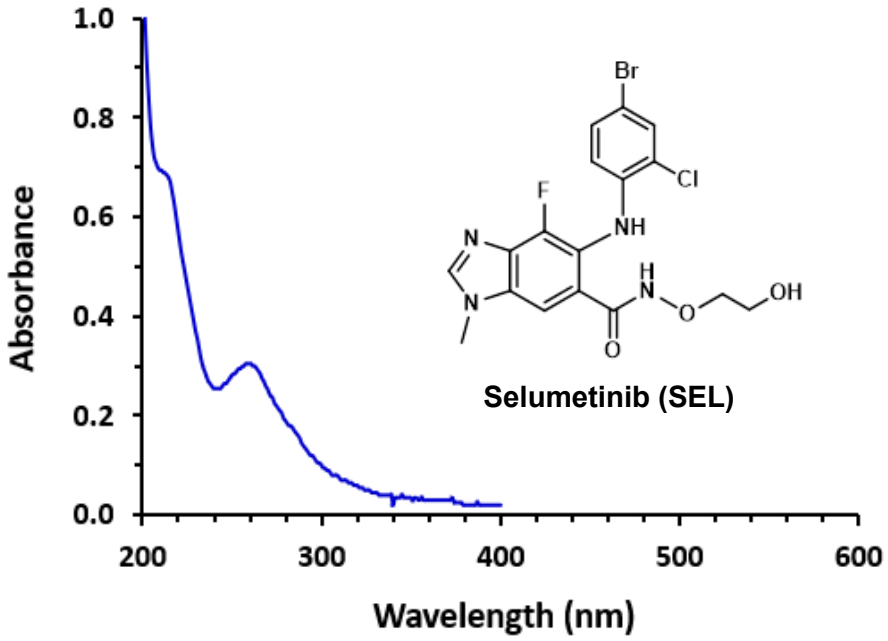

Fig. 1. The chemical structure of selumetinib (SEL) and the UV spectrum of its methanolic solution (50 µg mL^{-1}), at 255 nm.

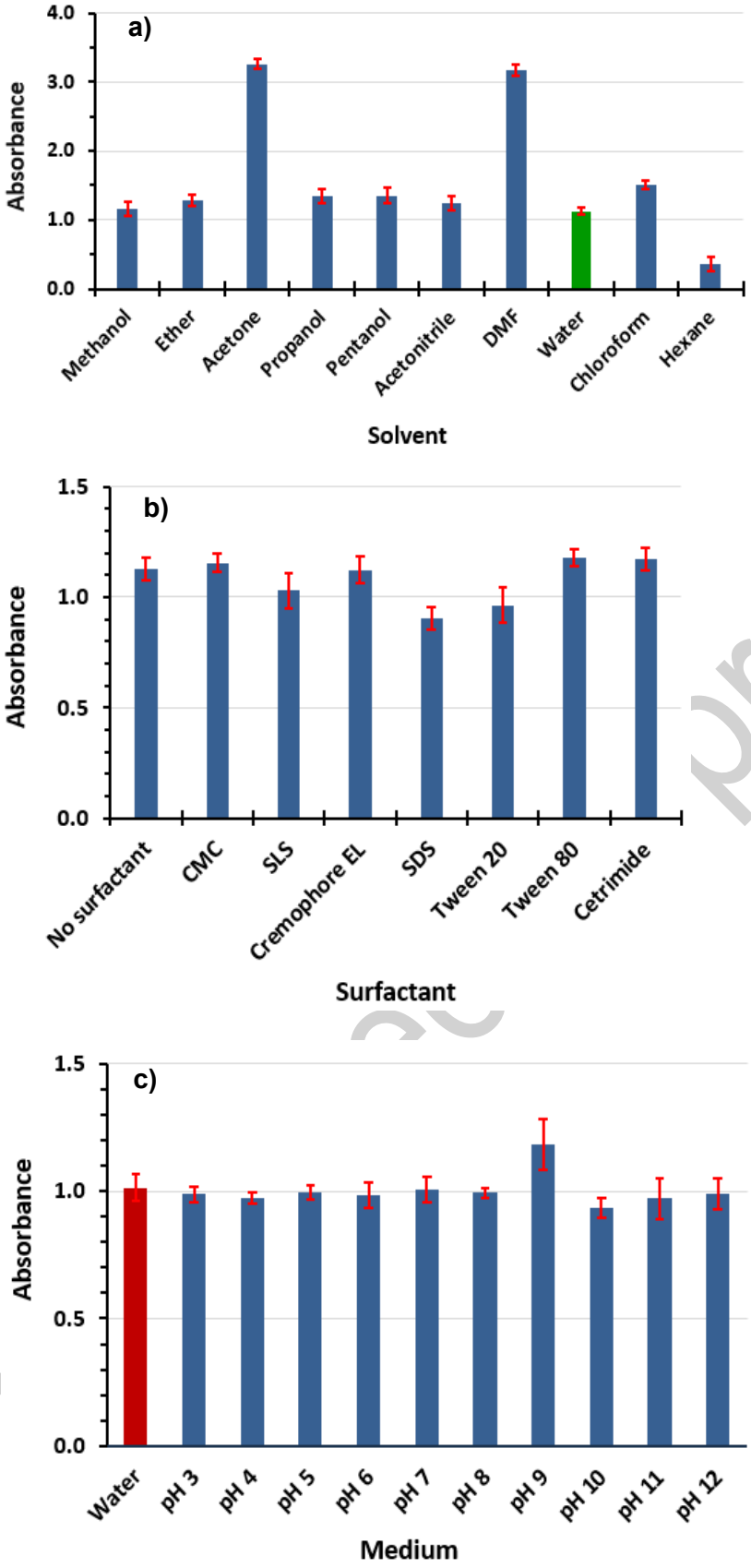

Fig. 2. The effect of: a) solvent, b) surfactant and c) pH of buffer, on UV absorption of SEL solution (50 µg mL^{-1}), at 255 nm. The values are average of 3 determinations ± SD.

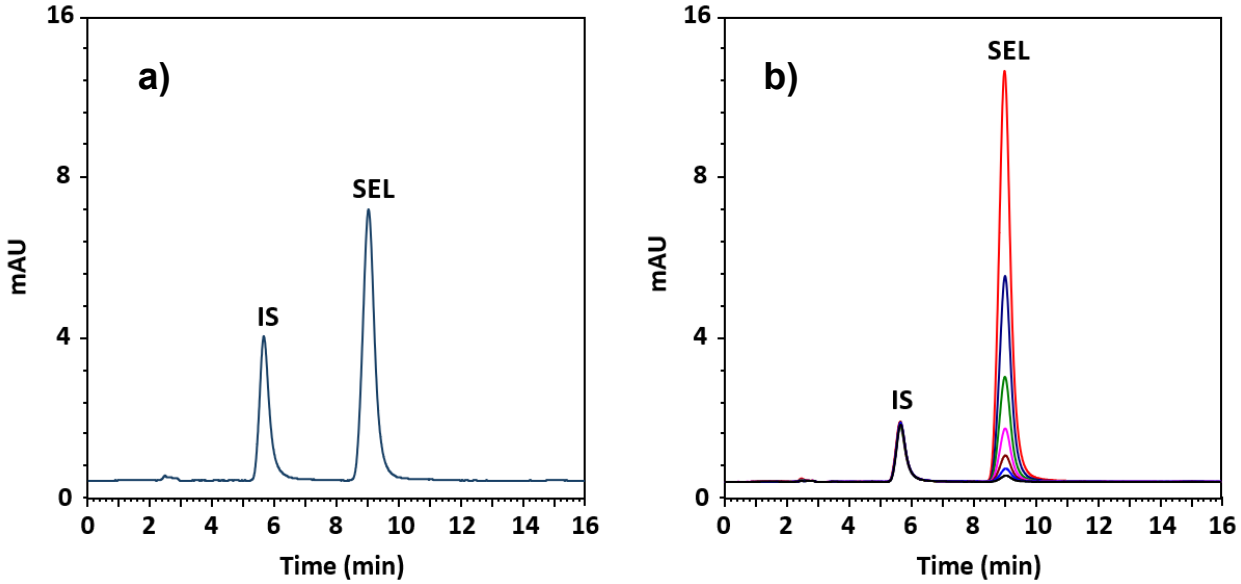

Fig. 3. Panel a): representative chromatogram of standard solutions of SEL (80 µg mL^{-1}) and TOZ solution (5 µg mL^{-1}) as an internal standard (IS). Panel b): overlaid chromatograms of varying concentrations of SEL standard solutions (0.8 – 100 µg mL^{-1}) containing a fixed concentration of IS (5 µg mL^{-1}). All measurements performed at 255 nm. mAU is the detector response in millivolts as arbitrary units.

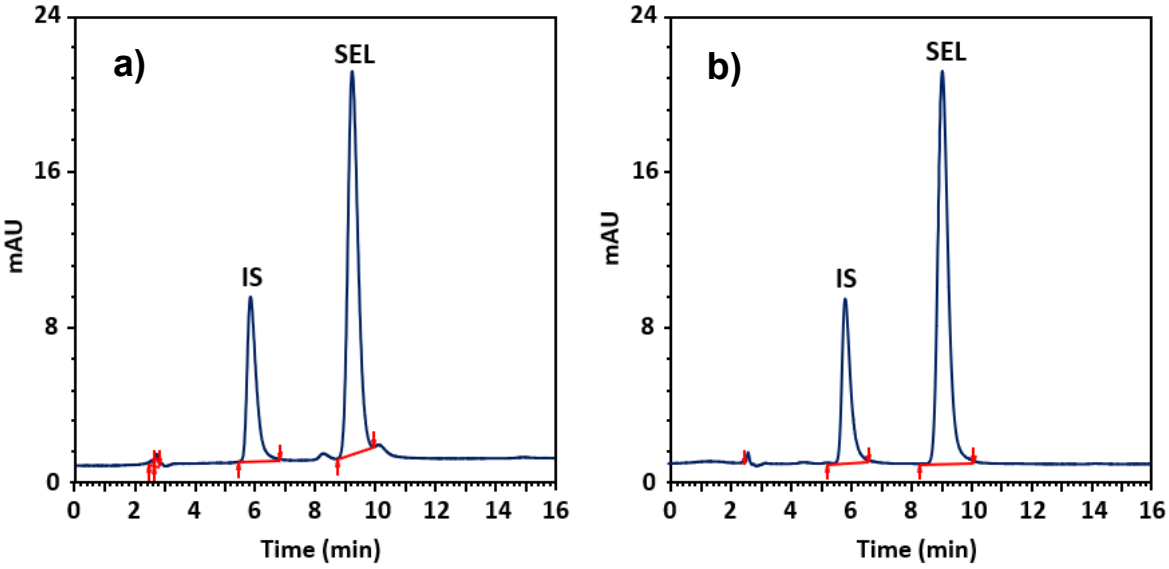

Fig. 4. Representative chromatograms of: a) standard solution of SEL, b) Koselugo® capsules solution. SEL standard solutions was 20 µg mL^{-1}, and expected concentration of SEL in Koselugo® capsules was also 20 µg mL^{-1} (IS: 5 µg mL^{-1}), at 255 nm. mAU is the detector response in millivolts as arbitrary units.

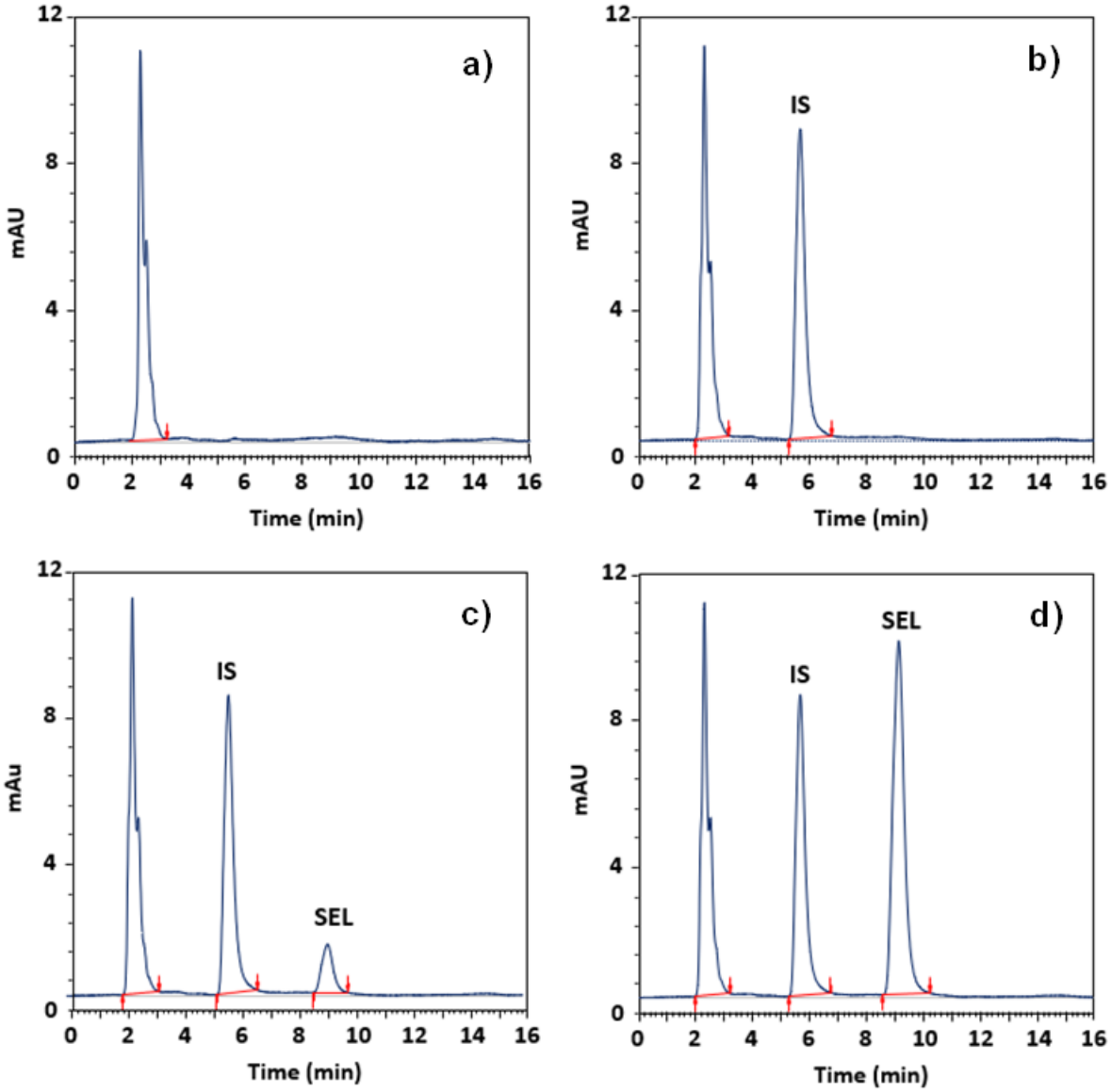

Fig. 5. Representative chromatograms of: a) blank SEL-free human plasma, b) blank plasma spiked with IS (5 µg mL^{-1}), c) blank plasma spiked with IS (5 µg mL^{-1}) and SEL at *LOQ* (3.46 µg mL^{-1}), d) blank plasma spiked with IS (5 µg mL^{-1}) and SEL (10 µg mL^{-1}). All measurements performed at 255 nm. mAU is the detector response in millivolts as arbitrary units.

a) GAPI tool

1. Sample collection/preparation
2. Sample preservation
3. Sample transport
4. Sample storage
5. Type of method: direct or indirect
6. Scale of extraction
7. Solvents/reagents used
8. Additional treatments
9. Reagent and solvents amount
10. Health risk
11. Safety risk
12. Instrumentation energy consumption
13. Occupational risk
14. Waste amount
15. Waste treatment

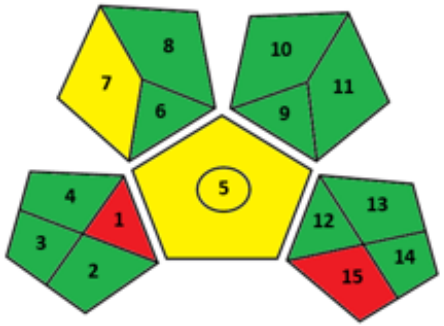

b) AGREE tool

1. Sampling procedure
2. Sample amount
3. Analytical device positioning
4. Sample preparation steps
5. Degree of automation
6. Derivatization agent
7. Amount of waste
8. Analysis throughput
9. Energy consumption
10. Source of reagent
11. Toxicity of reagents/solvents
12. Operator's safety

Fig. 6. The evaluation of the greenness of the proposed MW-UV and HPLC-PDA platforms for determination of SEL by a) GAPI and b) AGREE tools. The evaluation parameters and pictograms are given on the left-hand and right-hand section of each panel. The green color implies full adhesion to GAC; yellow & orange color implies moderate adhesion to GAC; red color implies no adhesion to GAC principles.